

Supporting Information

Flexible Vanadium-doped Ni₂P nanosheet arrays grown on carbon cloth for efficient hydrogen evolution reaction

Lulu Wen^{a,b}, Jie Yu^{a,b}, Changchang Xing^{a,b}, Dilong Liu^a, Xianjun Lyu^c, Weiping Cai^a and Xinyang Li^{a}*

^a Key Laboratory of Materials Physics and Anhui Key Laboratory of Nanomaterials and Nanotechnology, Institute of Solid State Physics, Hefei Institutes of Physical Science, Chinese Academy of Sciences, Hefei, 230031, China

^b University of Science and Technology of China, Hefei, 230026, China

^c Shandong University of Science and Technology, College of Chemical and Environmental Engineering, Qingdao, Shandong, 266510, China

* E-mail: xyli@issp.ac.cn

Experimental Section

Reagents

KOH, VCl_3 , $\text{Ni}(\text{NO}_3)_2 \cdot 6\text{H}_2\text{O}$, $\text{CO}(\text{NH}_2)_2$, $\text{NaH}_2\text{PO}_2 \cdot \text{H}_2\text{O}$, NH_4F , nitric acid (HNO_3), acetone and ethyl alcohol were bought from Aldrich or Sinopharm group. The chemicals were of analytical grade and used without further purification.

Synthesis of VNi-LDH/CC or $\text{Ni}(\text{OH})_2/\text{CC}$

The layered double hydroxide (LDH) nanosheet arrays grown on carbon cloth were prepared by hydrothermal process. In a typical synthesis, different molar ratios of V/Ni solution (0.1:3.9, 0.2:3.8, 0.4:3.6, 0.6:3.4, 0:4 for the synthesis of $\text{V}_{0.02}\text{Ni}_{0.98}$ -LDH/CC, $\text{V}_{0.05}\text{Ni}_{0.95}$ -LDH/CC, $\text{V}_{0.08}\text{Ni}_{0.92}$ -LDH/CC, $\text{V}_{0.15}\text{Ni}_{0.85}$ -LDH/CC and $\text{Ni}(\text{OH})_2/\text{CC}$, respectively) were obtained by mixing VCl_3 and $\text{Ni}(\text{NO}_3)_2 \cdot 6\text{H}_2\text{O}$ in 36 mL H_2O and the mixed solution was stirred 20 min to achieve a uniform solution, while the total amount of metal cations (V^{3+} and Ni^{2+}) were maintained at 4 mmol. Subsequently, NH_4F (8 mmol) and urea (15 mmol) were added, and the solution was stirred until a mixture solution is achieved. Meanwhile, the carbon cloth (1 cm \times 4 cm, CC) was sonicated in HNO_3 solution (3.0 mol/L) for 30 min to remove surface impurity, and then rinsed with acetone, distilled water, and absolute ethanol, and then dried in electric drying oven. Thereafter, the precursor solution was transferred to a 50 mL Teflon-lined autoclave. Then, a piece of pretreated carbon cloth was put into the reaction solution. The autoclave was sealed and placed in an electric oven and kept at 110 °C for 8 h. After the reaction, the autoclave was cooled down naturally. The sample was washed with distilled water and ethanol to remove the existed residuals

and then dried at 60 °C for 12 h in air.

Synthesis of V-Ni₂P NSAs/CC or Ni₂P NSAs/CC

In order to synthesis the V-doped Ni₂P nanosheet arrays, a low temperature phosphidation method were used here. In details, 200 mg of NaH₂PO₂·H₂O and as-prepared VNi-LDH nanosheet arrays were placed at two separate positions in a quartz boat inside a tube furnace under the Ar gas atmosphere. Afterwards, the furnace was heated up to 300 °C with a ramping rate of 2 °C min⁻¹ and kept for 2 h, and then cooled down naturally. As a contrast, the preparation process for Ni₂P nanosheet arrays on carbon cloth (VN_i LDH/CC) was similar to that for V-Ni₂P NSAs/CC except without addition of VCl₃.

Preparation of Pt-C/CC electrode

5 mg Pt-C, 250 μL ethanol, 250 μL H₂O and 20 μL nafion solutions were mixed and dispersed with ultrasonic for 30 min. An aliquot of 200 μL was pipetted onto the CC (1 cm²) for several times to reach a catalyst loading of 2.11 mg cm⁻².

Material Characterizations

The structures of the catalysts were measured through a high-resolution Philips X-Pert MRD X-ray diffractometer (XRD) with a Cu Kα radiation (λ=0.15419 nm). The morphology of the catalysts was revealed by a field emission scanning electron microscope (FESEM, Sirion 200) and transmission electron microscopy (TEM, JEOL, JEM-2010). The X-ray photoelectron spectroscopy (XPS) tests were conducted on an ESCALABMK II X-ray photoelectron spectrometer using Mg as the excitation source. The element distribution and atomic percentage were confirmed by energy dispersive

spectroscopy (EDS, Oxford Instrument and EDAX Inc.). Electron paramagnetic resonance (EPR) spectra were recorded using a Bruker EMX spectrometer (X band) at 77K (Bruker EMX plus 10/12). Ultraviolet photoelectron spectroscopy was performed by Thermo ESCALAB 250Xi, with photoelectron generated using 21.2 eV ultraviolet light from a He plasma discharge.

Electrochemical Measurements

Electrochemical measurements were performed on a CHI 760E electrochemical workstation (CH Instruments, Inc., Shanghai) with a standard three electrode system. Generally, a graphite rod, Ag/AgCl electrode and the prepared samples were used as the counter electrode, reference electrode and working electrode, respectively. For all tests, the SCE reference electrode was pre-calibrated with respect to a reversible hydrogen electrode (RHE). Before the electrochemical test, the system was degassed with nitrogen flow for 20 min to remove the dissolved oxygen. The continuous nitrogen flow was maintained throughout the electrochemical test. No activation was performed on the prepared samples before recording the polarization curves. The linear sweep voltammetry (LSV) tests were conducted in electrolyte at a scan rate of 2 mV s⁻¹. Electrochemical impedance spectroscopy (EIS) was performed to determine the interfacial charge-transfer resistance within the frequency range from 10 to 100 kHz in 1.0 M KOH solution. The amplitude of the alternating voltage was 5 mV.

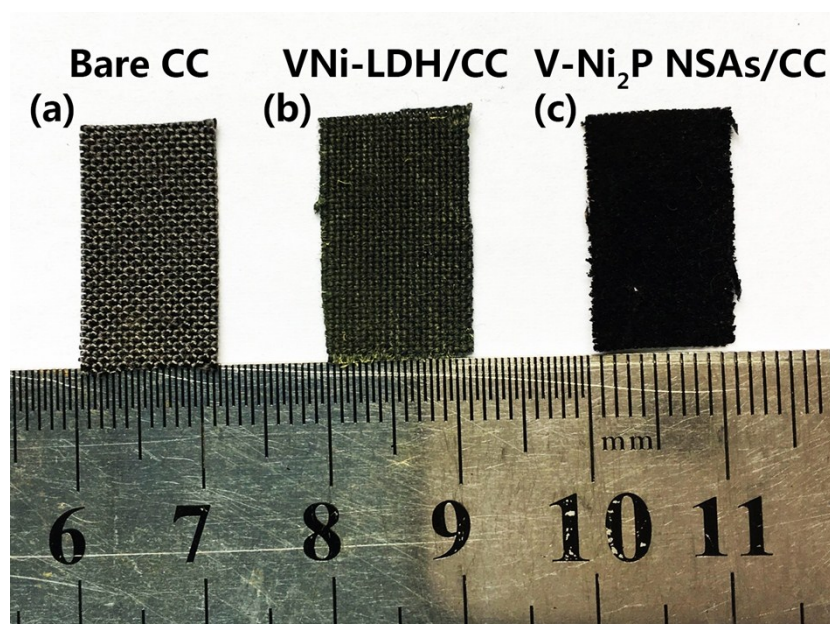


Figure S1. The photographic images of (a) carbon cloth (CC), (b) VNi-LDH/CC (c) V-Ni₂P NSAs/CC

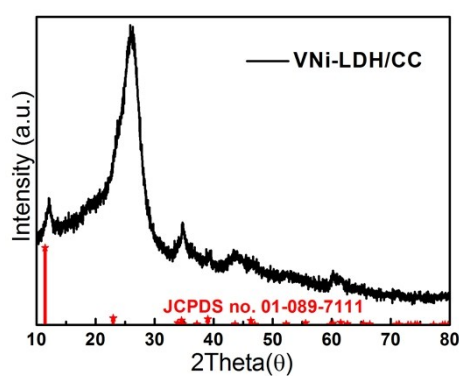


Figure S2. XRD pattern of VNi-LDH/CC precursor

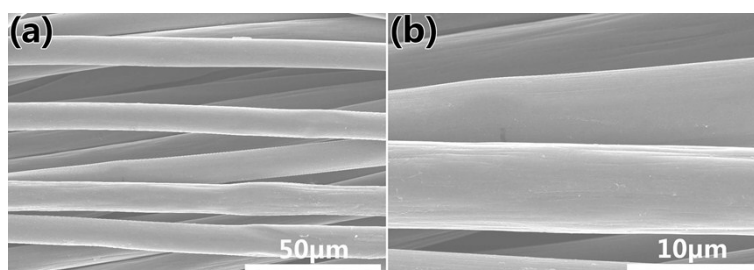


Figure S3. SEM images for bare CC (a) with low-magnification (b) with high-magnification.

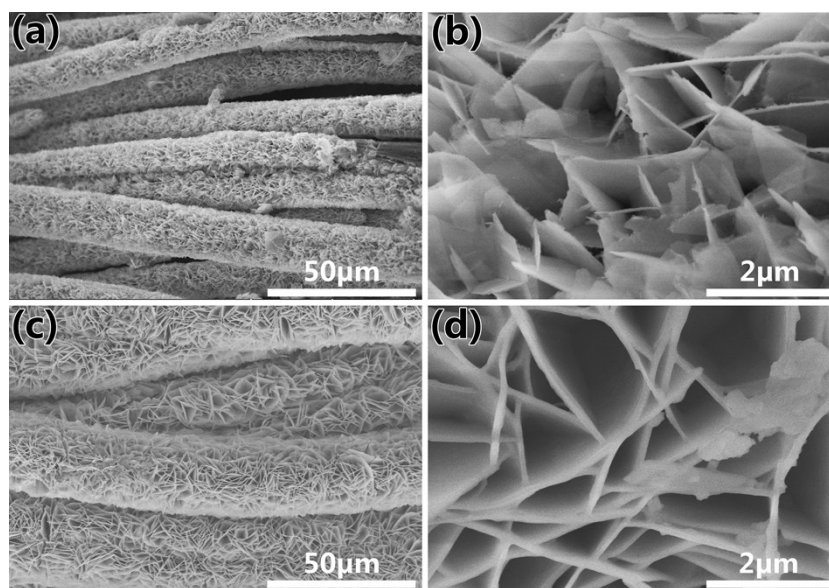


Figure S4. SEM images for Ni-LDH/CC (a) with low-magnification (b) with high-magnification. Ni₂P NSAs/CC (c) with low-magnification (d) with high-magnification.

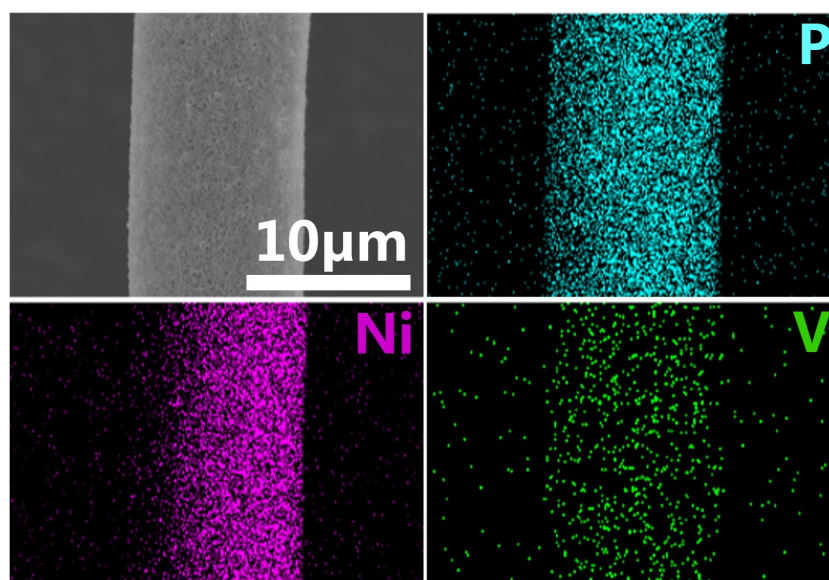


Figure S5. EDX elemental mapping of P, Ni, and V for V-Ni₂P NSAs/CC

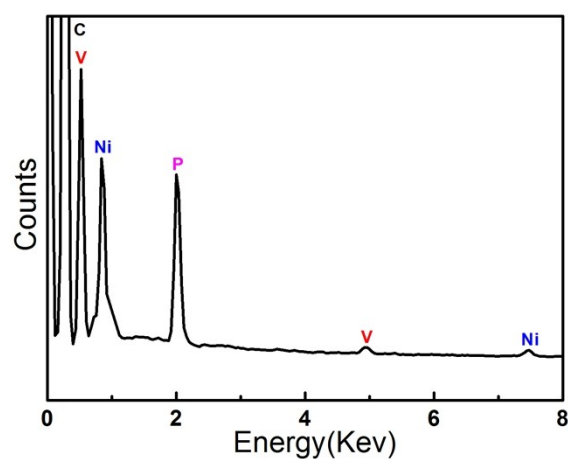


Figure S6. Energy dispersive spectroscopy spectrum of V-Ni₂P NSAs/CC

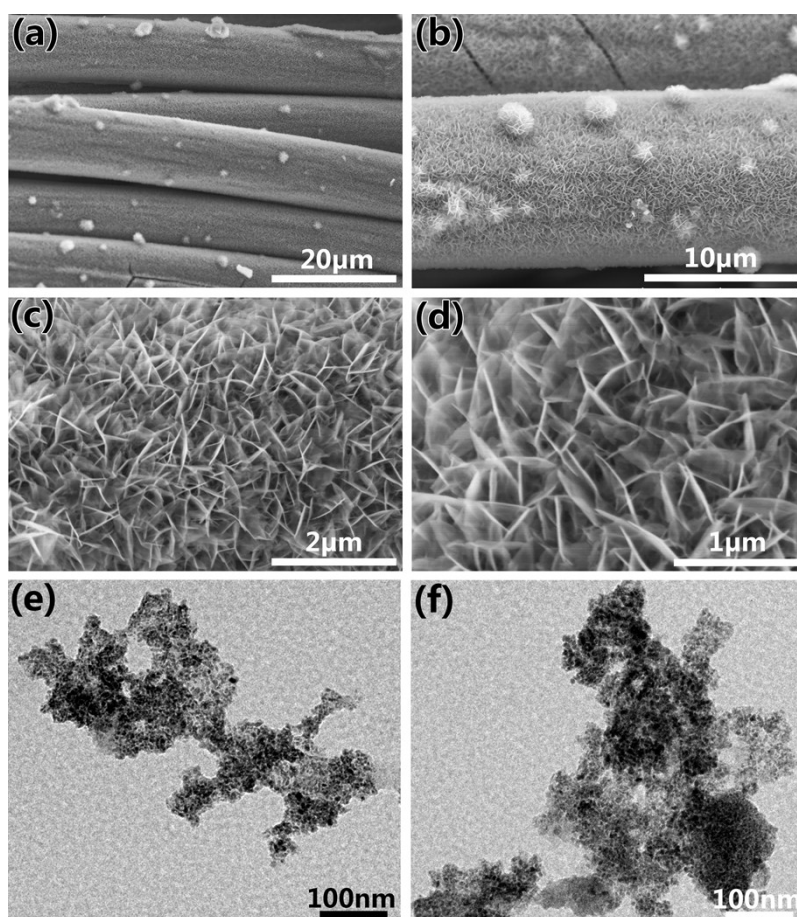


Figure S7. (a) Further morphology supplement of V-Ni₂P NSAs/CC: (a-d) SEM images of V-doped Ni₂P nanosheet arrays on CC with different magnification. (e-f) Corresponding TEM images.

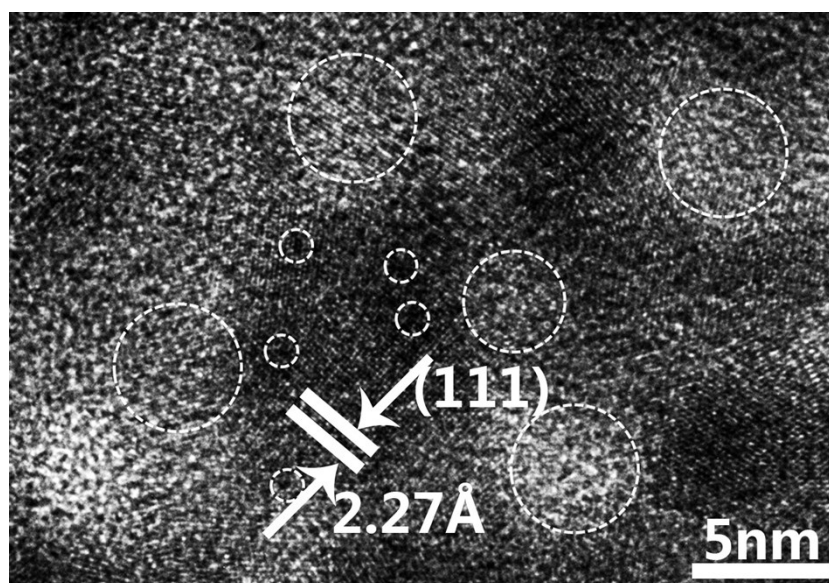


Figure S8. The enlarged High-resolution TEM (HRTEM) image of V-Ni₂P nanosheet

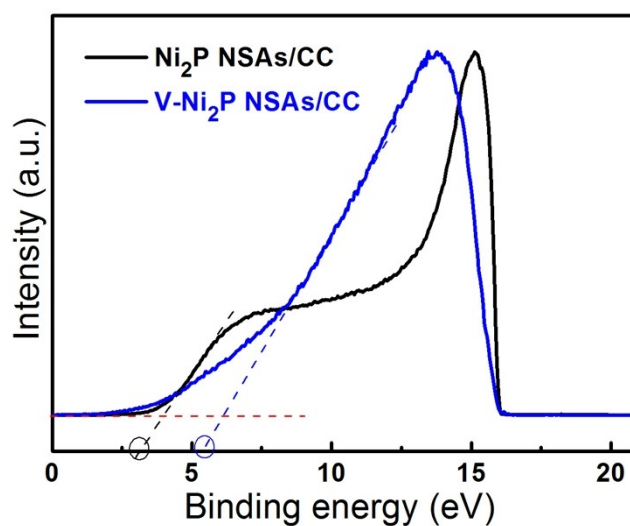


Figure S9. Ultraviolet photoemission spectrum (UPS) spectra of valence band for Ni₂P NSAs/NF and V-Ni₂P NSAs/NF.

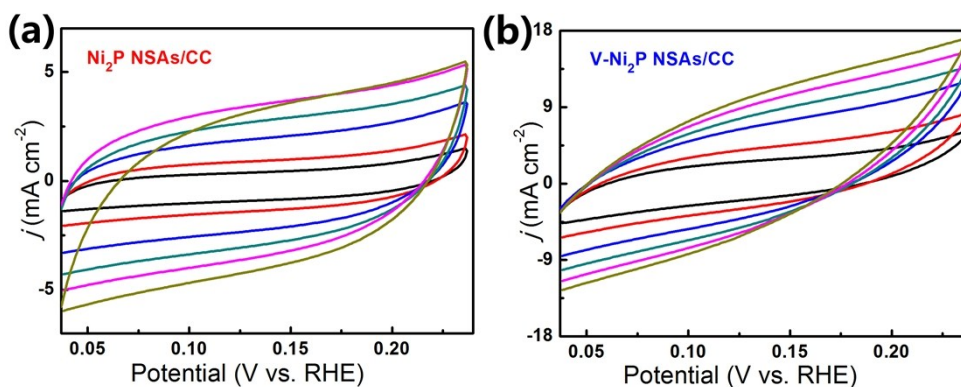


Figure S10. Cyclic voltammetry curves for (a) Ni₂P NSAs/CC (b) V-Ni₂P NSAs/CC in 1M KOH

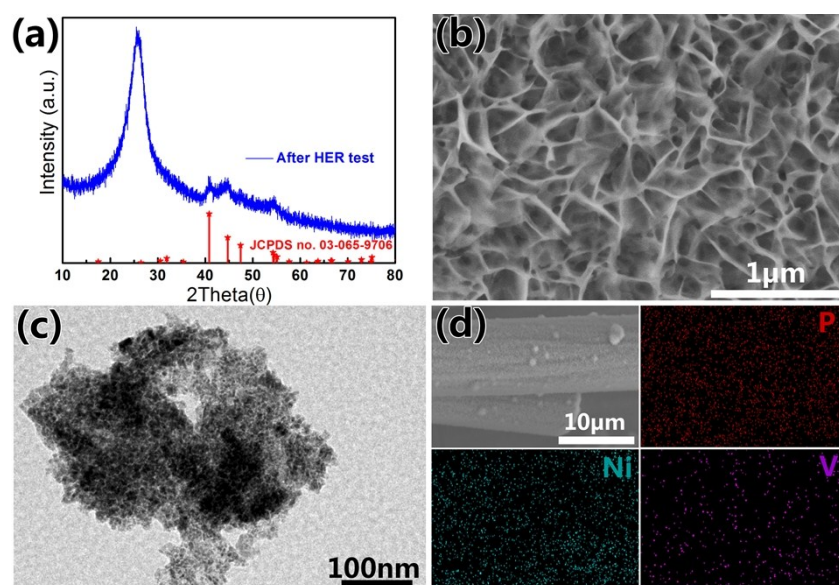


Figure S11. (a) XRD patterns of V-Ni₂P NSAs/CC after static overpotential for stability test 20 h in 1M KOH. (b) SEM image for V-Ni₂P NSAs/CC after static overpotential for stability test (c) Corresponding TEM images (d) Corresponding element mapping images of Ni, P, and V.

Table S1. Comparison of the HER performance of Cu-CoP NRAs/CC with other reported non-precious HER electrocatalysts in basic electrolyte.

Catalyst	Overpotential (10 mA cm ⁻²)	Electrolyte	Reference
V-Ni ₂ P NSAs/CC	85	1M KOH	This Work
Al-Ni ₂ P/TM	129	1M KOH	1
Ni ₂ P/CoN-PCP	94	1M KOH	2
Ni _{1.5} Fe _{0.5} P	282	1M KOH	3
Ni ₂ P@NF	114	1M KOH	4
NiCoP/N-rGO	115	1M KOH	5
Ni _{1.85} Fe _{0.15} P NSAs/NF	106	1M KOH	6
O ₃ -V10-Ni ₂ P	108	1M KOH	7
Ni ₂ P nanosheets	168	1M KOH	8
Ni/Ni ₂ P@3DNSC	92	1M KOH	9
NiS/Ni ₂ P/CC	111	1M KOH	10

REFERENCES

- [1] H. Du, L. Xia, S. Zhu, F. Qu and F. Qu, Chem. Commun., 2018, **54**, 2894-2897.
- [2] T. Sun, S. Zhang, L. Xu, D. Wang and Y. Li, Chem. Commun., 2018, **54**, 12101-12104.
- [3] H. Huang, C. Yu, C. Zhao, X. Han, J. Yang, Z. Liu, S. Li, M. Zhang and J. Qiu, Nano Energy, 2017, **34**, 472-480.
- [4] J. Zheng, W. Zhou, T. Liu, S. Liu, C. Wang and L. Guo, Nanoscale, 2017, **9**, 4409-4418.
- [5] X. Zhang, J. Li, Y. Sun, Z. Li, P. Liu, Q. Liu, L. Tang and J. Guo,

Electrochimica Acta, 2018, **282**, 626-633.

[6] P. Wang, Z. Pu, Y. Li, L. Wu, Z. Tu, M. Jiang, Z. Kou, I. S. Amiinu and S. Mu, ACS Appl. Mater. Interfaces, 2017, 9, 26001-26007.

[7] K. N. Dinh, X. Sun, Z. Dai, Y. Zheng, P. Zheng, J. Yang, J. Xu, Z. Wang and Q. Yan, Nano Energy, 2018, **54**, 82-90.

[8] Q. Wang, Z. Liu, H. Zhao, H. Huang, H. Jiao and Y. Du, J. Mater. Chem. A, 2018, **6**, 18720-18727.

[9] Y. Sun, T. Zhang, X. Li, Y. Bai, X. Lyu, G. Liu, W. Cai and Y. Li, Adv. Mater. Interfaces, 2018, **5**, 1800473.

[10] X. Xiao, D. Huang, Y. Fu, M. Wen, X. Jiang, X. Lv, M. Li, L. Gao, S. Liu, M. Wang, C. Zhao and Y. Shen, ACS Appl. Mater. Interfaces, 2018, **10**, 4689-4696.